

Study and Practice on Performance-based Seismic Design of Loess Engineering in China

Lanmin Wang¹, Jinchang Chen², Ping Wang¹, Zhijian Wu³, Ailan Che², Kun Xia¹

¹ Lanzhou Institute of Seismology, China Earthquake Administration, Lanzhou 730000, China

² School of Naval Architecture, Ocean and Civil Engineering, Shanghai Jiao Tong University, Shanghai 200040, China

³ College of Transportation Science and Engineering, Nanjing Tech University, Nanjing, Jiangsu 211816, China
wanglm@gdsdzj.gov.cn

Abstract. Loess is a kind of special soil with porous structure and weak cohesion, which widely deposits in China with an area of 640,000 km². Especially, it is continuously distributed in the Loess Plateau of China with an area of 440,000km² and a thickness ranging from tens meters to more than 500 meters, where is a region with the biggest thickness and the most complicated topography of loess deposit in the globe. On the other hand, the Loess Plateau is a strong earthquake-prone region, where 120 earthquakes with $M_s \geq 6.0$ and 7 events of $M_s \geq 8.0$ occurred in history. These earthquakes killed more than 1.4 million people in the region. The investigation shown that so large casualties should be attributed to a large scale of landslides, liquefaction, subsidence and amplification of ground motion. In this paper, the characteristics of engineering geology and seismic hazards with different probabilities of exceedance in the Loess Plateau of China is introduced. Based on the field investigation and exploration, observation data, in-situ tests, laboratory tests, and numerical analysis, the method of evaluating amplification of ground motion on topography and deposit of loess sites is proposed. The method of risk assessments of seismic landslides is developed. Seismic design for engineering loess slopes with single-step and multi-steps is provided. The methods of evaluating liquefaction and seismic subsidence of loess ground and its treatment measurements are respectively presented. Moreover, the seismic design methods of pile foundation in loess ground are proposed for considering the negative friction on piles due to seismic subsidence and horizontal pushing force on piles under liquefaction. The above-mentioned methods and techniques have been adopted by a national code and a provincial code, which have been proved to be practical, efficient and rational through a large number of major engineering projects and buildings' construction.

Keywords: Loess sites, seismic design, seismic landslides, liquefaction, subsidence, amplification.

1 Introduction

Earthquakes occur frequently in the loess region of China. By 2021, a total of 120 earthquakes with Ms6 or higher were recorded in the region, including 7 events with Ms8 and above. All of them have caused serious loess earthquake disasters such as seismic landslide, seismic subsidence and liquefaction, with more than one million casualties. In the former Soviet Union, the 1989 Tajikistan M 5.5 earthquake caused extensive liquefaction of saturated loess layer, resulting in large-scale mud flow, burying villages and killing 220 people. In the loess region of the Middle East of the United States, the New Madrid M 7.8 earthquake from 1887 to 1888 caused large-area liquefaction, land subsidence, and the Mississippi River poured into the subsided region to form a great lake. Table 1 presents some typical earthquake disaster examples in the loess area of China, which can be triggered under the effect of medium and strong earthquakes, resulting in huge casualties and property losses.

Table 1. Typical earthquake disasters in loess area

Time	Epicenter	Magnitude (Ms)	Maximum intensity	Main seismic geotechnical disasters	Casualties
1303	Hongtong, Shanxi Province	8	XI	Liquefaction, landslide and ground motion amplification	200,000
1556	Huaxian, Shaanxi Province	8	XI	Landslide, seismic subsidence, liquefaction and ground motion amplification	830,000
1654	Tianshui, Gansu Province	8	XI	Landslide, collapse and ground motion amplification	31,000
1659	Linfen, Shanxi Province	8	XI	Liquefaction, landslide and ground motion amplification	52,600
1718	Tongwei, Gansu Province	7.5	X	Landslide and seismic subsidence	40,000
1920	Haiyuan, Ningxia Province	8.5	XII	Landslide, liquefaction, seismic subsidence and ground motion amplification	270,000
1927	Gulang, Gansu Province	8	XI	Landslide, collapse and ground motion amplification	40,000
1995	Yongdeng, Gansu Province	5.8	VIII	Landslide, seismic subsidence and ground motion amplification	12
2013	Minxian, Gansu Province	6.6	VIII	Landslide, liquefied mud flow and ground motion amplification	95

The important progress of disaster research in loess area is that after the 1980s, the main research work was carried out in China, the United States, the former Soviet Union and Japan. From 1982 to 1998, a preliminary study on the liquefaction of loess in the central United States was conducted, and an in-depth study on the liquefaction standard, physical property index and particle size distribution of loess in this area was performed [1-3]. In 1990, Professor Ishihara of Japan conducted a detailed investigation and report on the liquefaction of saturated aeolian loess through the field investigation of large-scale mud flow caused by the M 5.5 earthquake in Tajikistan in 1989 [4]. In China, the research on the dynamic characteristics of loess mainly focuses on two respects. The first respect is the research on dynamic characteristics of loess, involving in elastic modulus, damping ratio, constitutive model, shear wave velocity and earth tremor according to the needs of site seismic zoning; The second respect is the research on seismic geotechnical disasters of loess, such as seismic landslide, seismic subsidence and liquefaction of loess. On the first respect, a lot of research on the stress-strain relationship, strength, elastic modulus and damping ratio of loess under constant amplitude sinusoidal cyclic loading on the dynamic triaxial apparatus have been done [5-9]; The dynamic constitutive model, elastic modulus, damping ratio and dynamic strength of loess under random seismic loading were widely studied [10-12], and the dynamic parameters of loess under different seismic loads were compared; The change law of loess strength under dynamic loadings were studied by means of laboratory simulated dynamic compaction tests [13]; The characteristics of shear modulus and damping ratio of loess in Northwest China were tested [14]. All these studies provide a lot of important data for the seismic microzonation of large and middle-sized cities in the loess region. On the second respects, field investigation and research on large-scale loess seismic landslide caused by the Haiyuan 8.5 earthquake in 1920 were conducted [15]. Aerial photos of large-area loess landslides caused by Tongwei earthquake in 1718 and Tianshui earthquake in 1654 were interpreted [16]. The seismic engineering geological problems of loess site was studied and the corresponding evaluation methods were put forward [17]. Seismic subsidence characteristics of undisturbed loess during humidification were studied [18]. The random search method to determine the most dangerous slip surface of loess slope was developed [19]. The prediction methods of seismic landslide, liquefaction and seismic subsidence of loess under random seismic loading were put forward [20-23]. A fuzzy comprehensive evaluation on the distribution law of landslides in Gulang and Haiyuan areas was made [24-26]. The intensity attenuation law and the development and distribution characteristics of seismic landslide and collapse in loess areas of China were studied [27]. The characteristics of high-speed sliding of loess landslide induced by earthquake were also studied [28]. The large-scale sliding of loess deposit caused by liquefaction of saturated loess layer during the Haiyuan 8.5 earthquake in 1920 was studied [29-30]. Experimental research on liquefaction potential of dynamic compacted loess ground and dynamic liquefaction of saturated loess were conducted [31-32]. The liquefaction of sand mixtures with different loess contents were studied [33]. It is found that the loess slows down or even prevents the dissipation of pore water pressure, which is caused by the large deformation and long-term high pore water pressure of fine-grained sand during liquefaction.

Although the above research works have achieved a lot of valuable research results in loess dynamics and seismic disasters in loess area, these results rarely involve seismic design of loess slopes and loess ground. However, the large-scale urbanization construction, infrastructure construction and construction of major engineering projects in the Loess plateau urgently need study the seismic design methods of loess engineering sites against seismic landslides, liquefaction, subsidence and amplification effect. In this paper, the authors present the methods of evaluating amplification of ground motion on topography and deposit of loess sites, assessing risk of seismic landslides, seismic design for engineering loess slopes with single-step and multi-steps, evaluating liquefaction and seismic subsidence of loess ground and its treatment measurements. seismic design of pile foundation in loess ground considering the negative friction on piles due to seismic subsidence and horizontal pushing force on piles under liquefaction. The achievements have been widely popularized and applied in the major engineering projects including high-speed railways, dams, airports in the loess region. The methods have been adopted by the National Standard for Seismic Design of Underground Structures (GB/T51336-2018) and the Seismic Design Code for Buildings in Gansu Province (GB62/T25-3055-2011).

2 Characteristics of engineering geology and seismic hazards in the Loess Plateau

2.1 Characteristics of engineering geology

Chinese loess area mainly distributed in the upstream and midstream of the Yellow River, involving in 7 provinces of Qinghai, Gansu, Ningxia, Shaanxi, Shanxi, Henan, Hebei, where is the Loess Plateau (Fig. 1). It has scattered distribution in other provinces. The thickness of loess ranges from tens meters to more than 500 meters with the most complicated topography of loess deposit in the globe.

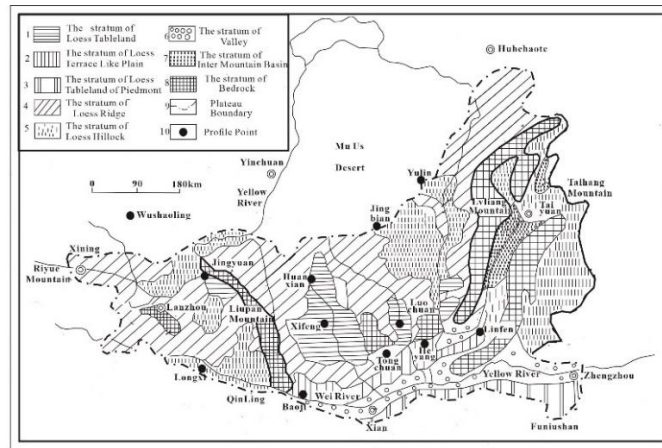


Fig. 1. Distribution of Loess Plateau and loess landforms (Teng, 1990)

The typical loess landforms in the Loess Plateau are mainly loess tableland, loess ridge, and loess round hill (Fig.2(a)(b)(c)). The microstructures of loess are respectively trellised porous structure, intergranular porous structure and coagulated porous structure from the western region, middle region, to eastern region of the Loess Plateau(Fig.2(d)). The former two structures have weak cohesion and the latter one has a little strong cohesion. The particles of loess are dominated by silt ranging from 60-70%. The other part is composed of sand and clay, which are 11%-3% and 18-29% respectively from the western region to eastern region of the plateau (Table 2). Such a special soil with porous microstructure, weak cohesion and silt dominated particles have a high vulnerability of seismic landslides, subsidence and liquefaction in the different landforms under the effect of strong earthquakes.

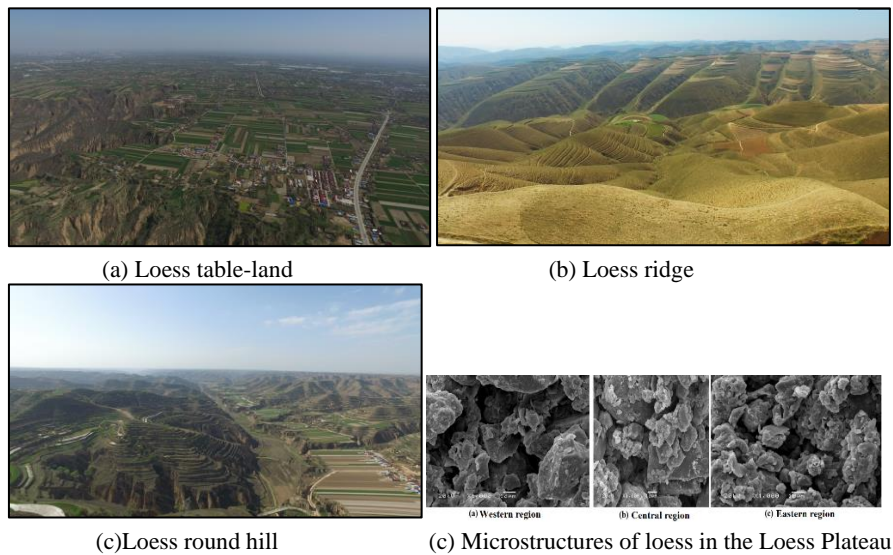


Fig. 2. The typical landforms and microstructures of loess in the Loess Plateau

Table 2. Particles Composition of loess in the difference regions

Sampling location	Sand	Silt	Clay
Western Region	10.94	70.92	18.14
Central Region	8.7	65.45	25.75
Eastern Region	3.8	67.1	29.10

2.2 Seismic hazards in the Loess Plateau

Factor superposition method is a common method for medium-scale disaster zoning, which has the advantages of clear significance and strong operability. There are many influencing factors of loess seismic disasters, but the influence degree of each factor on

disasters is not the same. Therefore, determining scientifically the weight of each influencing factor will make the zoning results more reasonable. In the compilation of this zoning map for the Loess Plateau, we adopted the method of factor weighted superposition. The steps of this method are :① Identification of factors affecting subsidence, liquefaction and landslide hazards; ② Figure digitization of influencing factors; ③ Classification assignment and weight determination of influence factors; ④ GIS weighted overlay analysis; ⑤ Classification of divisions; ⑥ Mapping. The work-flow diagram is shown in Fig. 3.

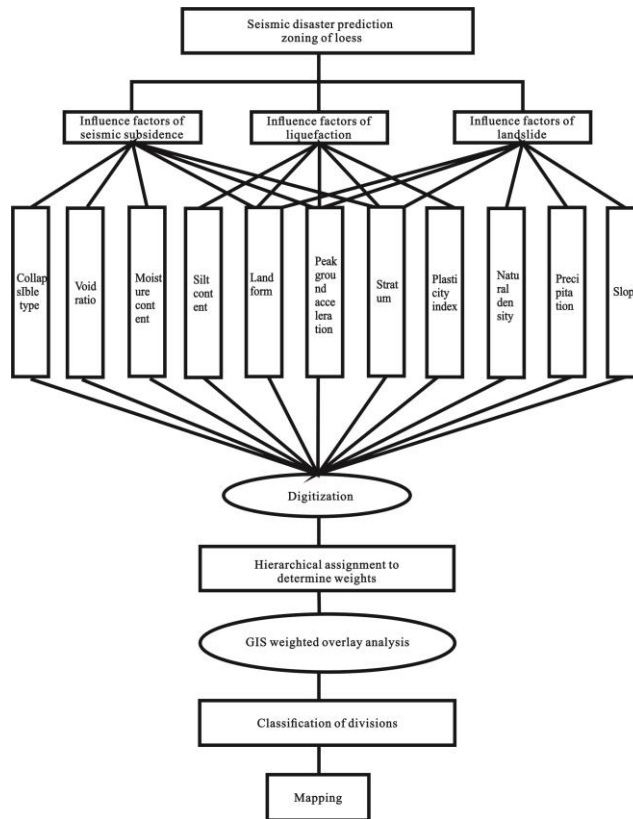


Fig. 3. Work flow diagram

Seismic landslide in Loess Plateau

When the exceedance probability in 50 years is 2% (Fig. 4(a)), serious landslides are mainly distributed near Tianshui, Haiyuan and Baiya. Moderate landslides are mainly concentrated in southern Ningxia and the eastern part of the Baiyin area, Tianshui area, the Weihe basin and around Taiyuan to Linfen. Mild landslides are distributed in the loess ridge and loess hill areas of the Loess Plateau. Non-landslide areas are mainly in the loess tableland.

When the exceedance probability in 50 years is 10 % (Fig. 4(b)), there is no serious landslide area. Moderate landslide areas are mainly distributed near Haiyuan and Tianshui. Mild landslides are mainly distributed in southern Ningxia, Baiyin, Tianshui, eastern and southwestern of Ordos block and Henan Province. The non-landslide area is mainly distributed in the Ordos block.

When the exceeding probability in 50 years is 63.5% (Fig. 3(c)), there is no serious landslide area. The moderate landslide area has sporadic distribution in Tianshui area. Mild landslide areas concentrate in Tianshui and southern Ningxia.

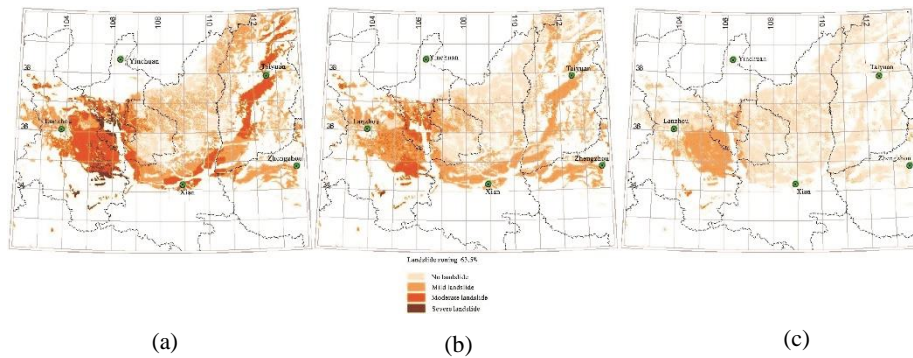


Fig. 4. Zoning maps of seismic landslides with different exceeding probabilities in 50 years ((a) 2%; (b) 10%; (c) 63.5%)

Seismic liquefaction in Loess Plateau

Since the liquefaction zoning is based on the assumption of loess saturated by underground water, rainfall water, and irrigation water, the liquefaction zoning results only represent the liquefaction potential, not the zoning results under the natural state.

When the exceeding probability in 50 years is 2% (Fig. 5(a)), there are mainly two regions with severe liquefaction potential. One is Tianshui to Huining area, the other is southern Ningxia and Jingyuan border area. It is also distributed near Gulang and Tianzhu in Gansu and Taiyuan in Shanxi. The areas with medium liquefaction potential are mainly distributed in the south of Ningxia, Tianshui area, Baiyin area, eastern part of Dingxi area, western part of Pingliang area. The areas with slight liquefaction potential are mainly located in the peripheral areas of the areas with medium liquefaction potential, and the area is large. The areas without liquefaction potential are mainly located in the northern part of Shanxi Province.

When the exceeding probability in 50 years is 10% (Fig. 5(b)), the area with serious liquefaction potential is distributed in Haiyuan area. The area with medium liquefaction potential is distributed in the south of Ningxia, east of Lanzhou, west of Liupan Mountain, and the belt area between Taiyuan and Linfen in Shanxi. The areas with slight liquefaction potential are mainly distributed in the eastern, western, southern margin of Ordos block and Henan province. Non-liquefaction potential areas are mainly distributed in Ordos block.

When the exceeding probability in 50 years is 63.5% (Fig. 5(c)), there is no severe liquefaction potential area and medium liquefaction potential area. The areas with slight liquefaction potential are mainly distributed in the south of Ningxia, the east of Lanzhou, the west of Liupan Mountain, and the northwest of Shanxi. There is also a small amount of distribution near Fuping in Shaanxi and Luoyang in Henan. Most loess areas have no liquefaction potential.

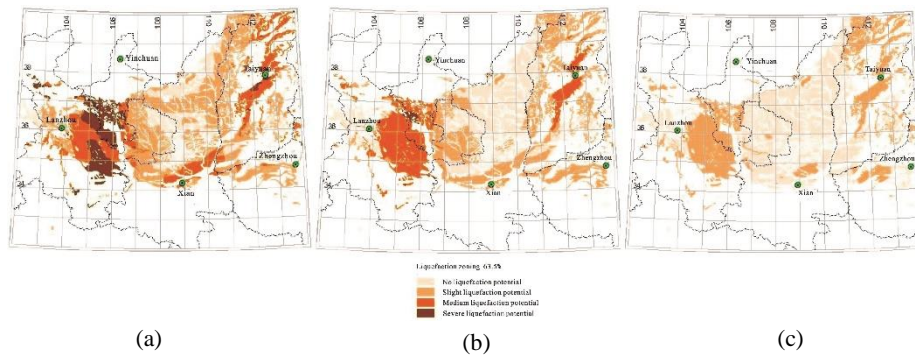


Fig. 5. Zoning maps of liquefaction potential with different exceeding probabilities in 50 years ((a) 2%; (b) 10%; (c) 63.5%)

Seismic subsidence in Loess Plateau

When the exceeding probability in 50 years is 2% (Fig. 6(a)), the areas with the most serious loess seismic subsidence disasters are near Tianshui City, Haiyuan and Guyuan at the junction of Ningxia and Gansu Province, which reach the level of Grade IV seismic subsidence with 60cm and above. The Grade III seismic subsidence area with 30-60 cm is distributed on the south of Ningxia and the southeast of Gansu. The Grade II seismic subsidence area with 7-30cm is widely distributed in the western edge, southern edge and eastern edge of the Ordos block, showing a zonal distribution. The Grade I seismic subsidence with less than 7cm and non-seismic subsidence area area is mainly distributed in the southern Ordos block.

When the exceedance probability in 50 years is 10% (Fig. 6(b)), the distribution of Grade III and Grade II seismic subsidence areas is roughly equivalent to that of Grade IV and Grade III seismic subsidence areas when the exceedance probability is 2 % in 50 years. Grade I seismic subsidence area is widely distributed in the east and west sides of Grade II seismic subsidence area. Non-seismic subsidence area is mainly distributed in the northern of Shaanxi.

When the exceedance probability in 50 years is 63.5% (Fig. 6(c)), there is no seismic subsidence hazards in the most areas.

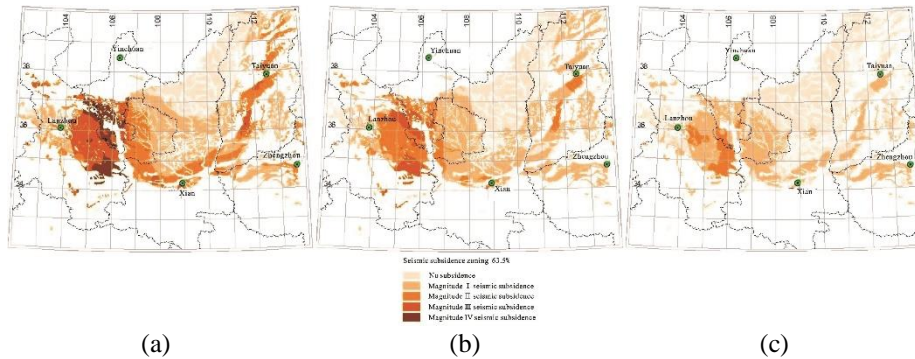


Fig. 6. Zoning maps of seismic subsidence with different exceeding probabilities in 50 years ((a) 2%; (b) 10%; (c) 63.5%)

Since ground motion, stratum and landform are the common influencing factors in seismic landslides, liquefaction and subsidence zoning and the dynamic vulnerabilities of loess in the different region of the plateau, the weight of ground motion appears mostly high. Therefore, the zoning of the three kinds of disasters have the similar overall trend. However, three kinds of disaster zoning have their own unique impact factors, so it will reflect differences in local distribution.

3 Seismic design methods of ground motion amplification

3.1 Field investigation

The Wenchuan Ms8.0 earthquake in 2008 not only had a great influence on structures near the fault area, but also made a significant impact on the loess tableland far from the epicenter due to predominate amplification of ground motion. In Gansu Province, Dazhai Village in Pingliang City is located at the top of the 100-meter-thick loess plateau platform where is 500 km away from the epicenter. The houses in the village are mainly wooden structures, masonry structures and adobe structures. 70% of the houses collapsed or seriously damaged during the earthquake and the seismic intensity reached their fortification intensity of VII degree, which is 1 degree higher than that of the area below the tableland where the houses were in good condition (Fig. 7).



Fig. 7. The seismic intensity is VII-degree at Dazhai village on the loess tableland

3.2 On-site observation

After the Wenchuan main shock, the investigation team monitored the ground motion on the slope of a loess tableland edge in Wenxian County, Gansu Province ("Wenxian tableland slope" for short) (Fig 8). The gradient of Wenxian tableland slope is $35^\circ \sim 45^\circ$ and the relevant height is about 50 m. Three observation stations of strong ground motion were set up in different locations of the slope with basically the same geological conditions: station-1 at the bottom of slope (N32.94°, E104.70°, altitude is 927 m), station-2 at the middle of slope (N32.95°, E104.67°, altitude is 960 m) and station-3 at the top of slope (N32.94°, E104.67°, altitude is 969 m). The recorded PGA of the aftershocks and related information are shown in Table 3. The observation station at the bottom of the slope was selected as the reference station to analyze the amplification effect of slope on the loess tableland. Totally 9 aftershocks were recorded at the observatory stations. The time histories of ground motion shown that the amplification coefficient of horizontal peak ground acceleration ranges from 1.1-2.7 with the magnitudes of Ms4.1-5.7.

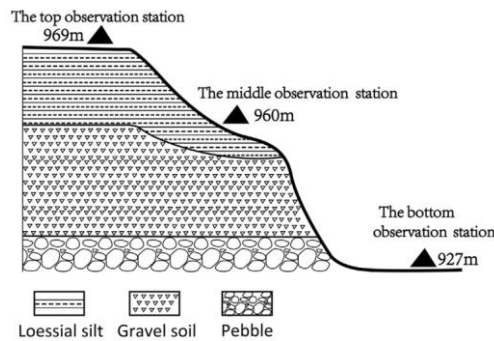


Fig. 8. The temporary strong motion observation array near the Wenxian County

In addition, the analysis on the recorded time histories of peak ground motion of the Wenchuan Ms8.0 mainshock at 4 observatory stations with a distance of 65km and 120km away from the epicenter shown that the amplification coefficient of horizontal peak ground acceleration due to loess deposit is 1.3 and 4.1 respectively. The recorded data of the Mixian-Zhangxian Ms6.6 earthquake at the same 4 stations shown that the amplification coefficient due to loess deposit is 2.1 and 5.0 respectively.

3.3 The seismic design method of PGA amplification

In order to evaluate the amplification effect of loess deposit thickness and slope height on ground motion, a series of large-scale shaking-table tests and numerical simulations were carried out. Furthermore, the seismic design method of PGA amplification is proposed based on the field investigation, observation data, shaking-table tests and numerical simulation comprehensively. The design PGA and characteristic period at engineering sites with different loess thickness may be respectively determined by the

local fortification PGA plus an amplification coefficient shown as Table 3 and Table 4. The design PGA at engineering slope sites with relevant height of 50m and above may be determined by the local fortification PGA plus an amplification coefficient for different slope angles shown as Table 5. The characteristic period at engineering slope sites with relevant height of 50m and above may be determined by Table 4, in which the relevant height of slope is equivalent to thickness of loess.

Table 3. The amplification coefficient of PGA with different thicknesses of loess sites.

Thickness/m	20	40	60	80	100	120	160	200	≥240
≤0.05g	1.1	1.2	1.3	1.3	1.3	1.4	1.4	1.5	1.6
0.10g	1.1	1.1	1.2	1.2	1.2	1.3	1.3	1.4	1.4
0.15g	1.05	1.05	1.1	1.1	1.1	1.2	1.2	1.2	1.2
0.20g	1	1.05	1.05	1.05	1.05	1.1	1.1	1.1	1.1
0.30g	1	1	1	1	1	1	1.05	1.05	1.05
≥0.40g	1	1	1	1	1	1	1	1	1

Table 4. Characteristic periods (s) adjusted with different thicknesses of loess site.

Thickness/m	20	40	60	80	100	120	160	200	≥240
≤0.05g	0.54	0.63	0.69	0.7	0.7	0.7	0.7	0.7	0.75
0.10g	0.55	0.64	0.69	0.7	0.7	0.7	0.7	0.7	0.75
0.15g	0.57	0.65	0.69	0.7	0.7	0.7	0.7	0.7	0.75
0.20g	0.59	0.67	0.69	0.7	0.7	0.7	0.7	0.75	0.75
0.30g	0.61	0.68	0.7	0.7	0.7	0.7	0.7	0.75	0.75
≥0.40g	0.63	0.69	0.7	0.7	0.7	0.7	0.7	0.75	0.75

Table 5. Amplifying factor with loess slope effects

Slope (50m high)	20°~30°	30°~45°	45°~60°	60°~70°
PGA amplifying factor	1.1-1.3	1.3-1.5	1.5-1.7	1.7-2.0

4 Seismic design of engineering slopes of loess

Based on the investigation of a large number of loess seismic landslides, the prediction and calculation of the maximum sliding distance and disaster range of loess seismic landslides, and considering the amplification effect of slope ground motion, the seismic safety design method of loess slope is developed.

When the high-rise building is located at the slope crest, the distance between the building and the edge of the slope crest should not be less than 20m; The distance between the edge of the foundation slab and the edge of the slope bottom shall not be less than 1.25 times of the slope height below the foundation slab (H_1). See Fig. 9(a) In the figure, d is the buried depth of the foundation.

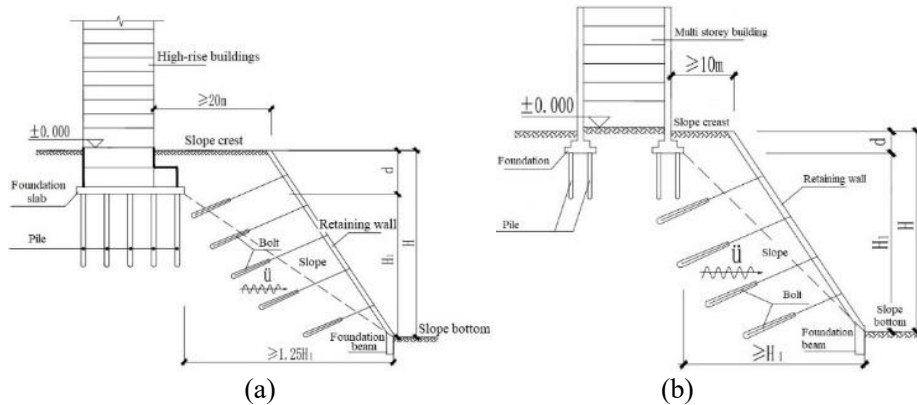
When the multi-storey building is located at the crest of the slope, the distance between the building and the edge of the slope crest should not be less than 10m; The

distance between the base edge and the slope bottom edge should not be less than the slope height below the base (H_1). See Fig. 9(b).

When multi-storey and high-rise buildings are located at the slope bottom, the distance between the buildings and the edge of the slope bottom should not be less than 10m, as shown in Fig. 9(c).

When the high-rise building is located on the platform in the middle of the slope and the ground height difference on both sides of the building is no more than 4.5m and no more than 1 floor, the distance from the building to the bottom edge of the upper slope should not be less than 10m; The distance from the edge of the lower slope crest to the bottom edge of the lower slope should not be less than 20m; The distance between the edge of the foundation slab and the bottom edge of the lower slope should not be less than 1.25 times of the slope height below the foundation slab (H_1); No building shall be stacked or set within 20m from the top edge of the upper slope; The surface soil layer of the lower slope shall be compacted. See Fig. 9(d).

When the high-rise building is located on the platform in the middle of the slope, and the ground height difference on both sides of the building is no more than 12m and no more than 3 floors, in addition to meeting the above requirements, the following requirements shall also be met: The distance between the edge of the foundation slab and the bottom edge of the lower slope should not be less than 1.5 times of the slope height below the foundation slab (H_1); Permanent support facilities shall be set at the bottom of the upper slope near the outside of the building, and the design service life of the support facilities shall not be less than the service life of the building, and must be separated from the building; The deformation joint below the embedded end shall be backfilled tightly, and the space above the embedded end shall be left blank or other measures that will not affect the displacement of the building shall be taken. See Fig. 9(e).



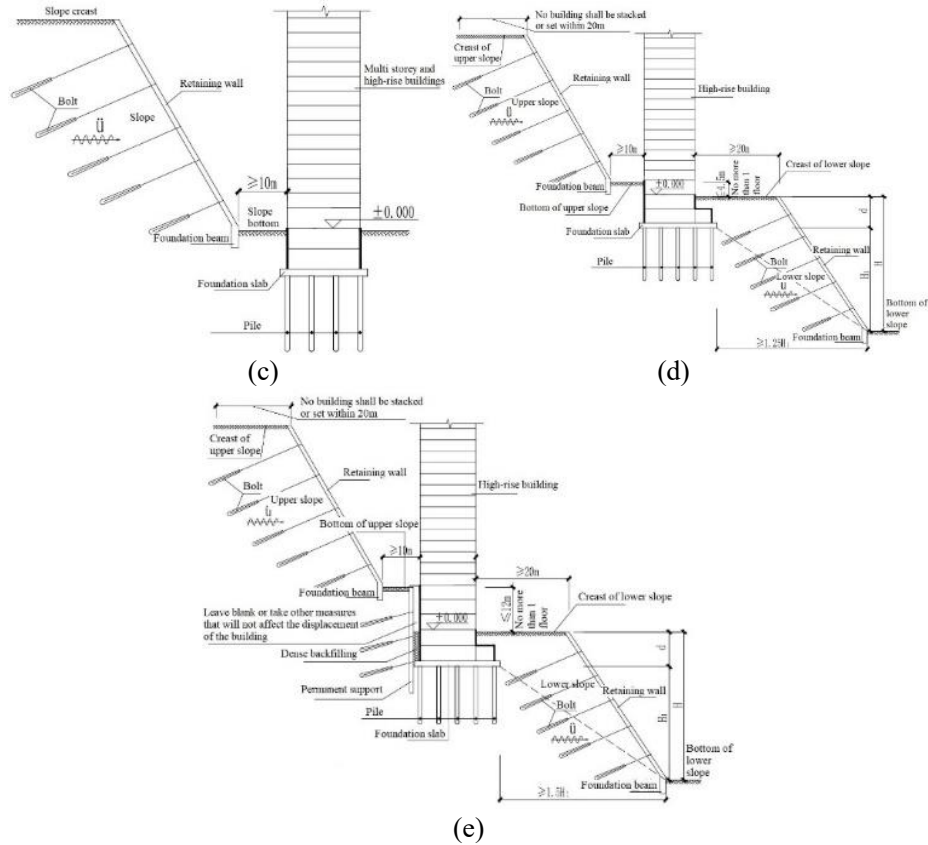


Fig. 9. Schematic diagram of seismic design of Engineering Slope

The above research results have been fully adopted by the code 'Specification for seismic design of buildings' in Gansu Province (GB62/T25-3055-2011)(2021 revised version), in which the first author is one of chief editors.

5 Evaluation and prevention of liquefaction of loess ground

5.1 Preliminary discrimination method

Based on the evaluation of factors affecting loess liquefaction including soil saturation, soil depth, sedimentary age, particle composition, physical property, and microstructure type, we proposed the preliminary discrimination method of liquefaction potential of loess ground with engineer practicality. When saturated loess (including loess-like soil) meets one of the following conditions, it can be preliminarily judged as non-liquefaction circumstance or that the impact of liquefaction may not be considered.

(1) When the geological age is the early Middle Pleistocene loess (Q_2^1) and before, it can be considered that no liquefaction would occur at seismic intensity of VII (0.15g) VIII (0.20g, 0.30g) and IX (0.4g) degree.

(2) Loess with saturation less than 60%.

(3) When the content percentage of clay particles (particle size $<0.005\text{mm}$) of loess is not less than 12%, 15%, and 18%, the impact of liquefaction may be ignored at seismic intensity of VII, VIII, and IX degree respectively.

(4) For buildings with shallow buried natural foundation, when the thickness of overlying non-liquefied soil layer and the depth of groundwater level meet one of the following conditions, the impact of liquefaction may be not considered:

$$d_u > d_0 + d_b - 2$$

$$d_w > d_0 + d_b - 3$$

$$d_w + d_u > 1.5d_0 + 2d_b - 4.5$$

where, d_u (m) is thickness of overlying non-liquefied soil layer (excluding silt and mudding soil layer); d_w (m) is depth of groundwater level, taken as the annual average maximum water level within the design reference period or the recent annual maximum water level; d_b (m) is buried depth of foundation, taken as 2 m if less than 2 m; d_0 (m) is characteristic depth of loess liquefaction.

5.2 Detailed discrimination method

The research on detailed discrimination method of saturated loess ground liquefaction involves liquefaction shear stress ratio, liquefaction index, microstructure characteristic parameter, and SPT (standard penetration test) counts. Herein detailed discrimination standard is discussed based on the SPT counts.

The results of frequentness statistics of SPT counts in saturated loess sites are shown in Fig. 10(a). It can be seen that about 50% of the sites have SPT counts lower than 6, while 85% of the sites have SPT counts lower than 9, and only 16% of the saturated loess sites have SPT counts higher than 9.

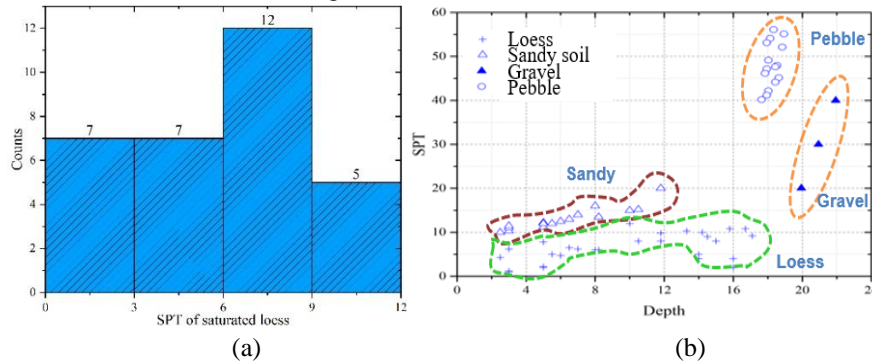


Fig. 10. (a) SPT counts frequentness histogram of saturated loess sites; (b) SPT counts of different saturated sites

The SPT counts of saturated loess and other saturated soils are further compared, and the SPT counts of different saturated sites is shown in Fig. 10(b). It can be noticed that the SPT counts increases from loess to sandy soil, gravel, and pebble. The SPT counts of loess is close to that of sandy soil, but there are still obvious differences between them. The SPT counts value of different saturated soils is listed in Table 6.

Table 6 SPT counts of different saturated soil

Soil	Minimum SPT counts	Maximum SPT counts	Average SPT counts
Loess	1.8	12	6.3
Sandy soil	10	21	13.1
Gravel	20	40	30
Pebble	39	55	47.4

The average SPT counts of saturated loess is 6.3, while that of saturated sandy soil is 13.1, which is approximately twice the difference. However, it will become easy for engineers to make the detailed discrimination of loess liquefaction if we still use the discrimination formula of sand liquefaction from the national code with the reference value of SPT counts of saturated loess.

In National Code for Seismic Design of Buildings, the critical value of SPT counts for sand liquefaction discrimination within 20m depth is calculated as formula (1):

$$N_{cr} = N_0 \beta [\ln(0.6d_s + 1.5) - 0.1d_w] \sqrt{3/\rho_c} \quad (1)$$

Where, N_{cr} is critical value of SPT counts for liquefaction discrimination; N_0 is reference value of SPT counts for liquefaction discrimination; d_s (m) is SPT depth of saturated soil; d_w (m) is depth of groundwater level; ρ_c is percentage of clay content, taken as 3 if less than 3 or sandy soil; β is adjustment coefficient, taken as 0.80 for seismic design first group, 0.95 for seismic design second group, and 1.05 for seismic design third group.

The comparative results of field test and laboratory test show that formula (1) is applicable to the discrimination of liquefaction potential of natural saturated loess, but the reference value of SPT counts needs correction. Table 7 provides the reference value of SPT counts for loess liquefaction discrimination.

Table 7 Reference value of SPT counts for loess liquefaction discrimination

Seismic design acceleration (g)	0.10	0.15	0.20	0.30	0.40
Reference value of SPT					
National code	7	10	12	16	19
Provincial specification	7	8	9	11	13

The comparison between measured SPT counts and calculated critical value of SPT counts for liquefaction discrimination is shown in Fig. 11.

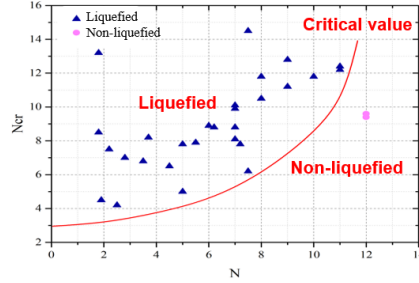


Fig. 11. Comparison between measured SPT counts and calculated critical value of SPT counts for liquefaction discrimination

For the saturated loess ground defined by Formula (1), the liquefaction index of each borehole can be calculated using Formula (2) to comprehensively divide the liquefaction grade of ground.

$$I_{IE} = \sum_{i=1}^n \left[1 - \frac{N_i}{N_{cri}} \right] d_i W_i \quad (2)$$

Where, N_i is SPT counts of soil layer; d_i is thickness of soil layer; N_{cri} is critical value of SPT counts for liquefaction discrimination; W_i is depth weight, calculated using Formula (3):

$$W_i = \begin{cases} 10 & (d_s < 5\text{m}) \\ \frac{10}{3} \cdot d_s - \frac{20}{3} & (5 < d_s \leq 20) \end{cases} \quad (3)$$

According to the result of Formula (2), the liquefaction characteristics of loess site can be determined by the comprehensive classification standard of liquefaction potential of natural loess given in Table 8.

Table 8 Classification standard of liquefaction potential of natural loess

Liquefaction grade	Slight	Medium	Serious
Liquefaction index (I_{IE})	$0 < I_{IE} \leq 6$	$6 < I_{IE} \leq 18$	$I_{IE} > 18$

5.3 Technology and standard of anti-liquefaction treatment of loess ground

Dynamic compaction method (DCM)

Dynamic compaction ground of 330kV Dongjiao substation in Lanzhou is selected as the research subject. The liquefaction resistance performance of loess ground before and after dynamic compaction is studied. The site is in Liugouping, 500m east of Taoshuping, Donggang Village, Lanzhou.

The curve of strain and pore pressure during loess liquefaction after DCM are shown in Fig. 12. The loess after dynamic compaction still has large dynamic strain. Although pore pressure ratio is only about 0.5, when pore pressure increases to the maximum, the

strain growth accelerates suddenly. Therefore, the loess ground after DCM still has a certain liquefaction potential.

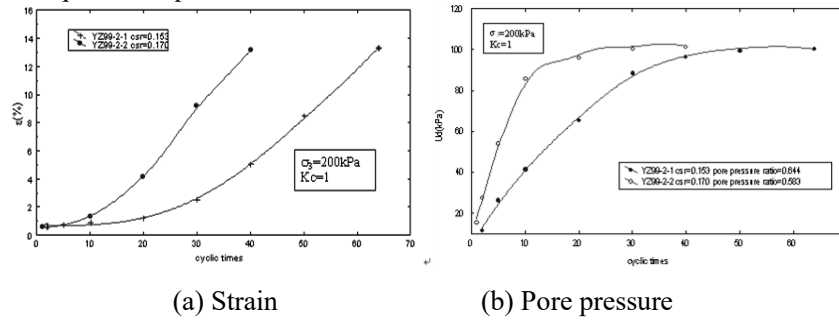


Fig. 12. Curve of strain and pore pressure during loess liquefaction after DCM

The dry density and liquefaction stress ratio of ground soil are improved after DCM. Due to the close relation between loess liquefaction and the characteristics of particle composition and structural cementation in loess, although DCM can not eliminate the liquefaction potential of loess, it is of positive significance to improve the liquefaction resistance of loess ground. Other anti-liquefaction measures should be considered in combination with DCM to ensure the safety of buildings in engineering activities.

Compaction pile method (CPM)

Research site is the primary school of Lanzhou Refinery and lime soil CPM is used for ground treatment. After lime soil CPM treatment, the dry density of ground soil has been improved, generally more than 1.53g/cm^3 , with an average of 1.58g/cm^3 . To study the effect of lime soil CPM on reducing the liquefaction potential of loess ground, dynamic triaxial liquefaction tests are conducted on soil samples taken before and after treatment, and test results are shown in Fig. 13.

Results show that lime soil CPM is effective in dealing with the collapsibility of loess, but there is limitation in reducing the liquefaction potential of loess ground. After lime soil CPM treatment, the liquefaction stress ratio of loess ground is improved, and the average liquefaction stress ratio of loess sample after treatment is twice that before treatment. Therefore, it can be considered that lime soil CPM can increase the liquefaction stress ratio of loess by about 0.1-0.2.

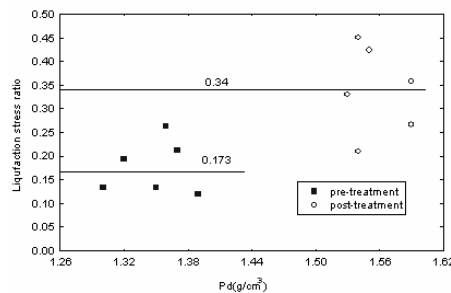


Fig. 13. Variation of liquefaction stress ratio before and after lime soil CPM treatment

Above calculation indicates that the liquefaction triggering seismic intensity of loess ground after treatment can be increased by more than one degree compared with that before treatment. However, under the seismic intensity of VIII degree and above, the loess ground treated with lime soil CPM still has the possibility of liquefaction. Lime soil CPM treatment can not eliminate liquefaction potential of loess ground, but it can improve the liquefaction resistance of loess ground.

In conclusion, the liquefaction potential of saturated loess ground can be reduced or eliminated using DCM or lime soil CPM treatment under condition of seismic intensity less than VIII degree. Anti-liquefaction performance of ground soil depends on the compactness of ground soil after treatment. The above treatment methods can be approximately selected according to the importance of construction project. Under the condition of seismic intensity of IX, compaction treatment can enhance the liquefaction resistance of loess ground, but it has a certain limitation on eliminating liquefaction potential of saturated loess ground. For important buildings or projects, some other treatment (like chemical grouting) should be adopted in combination with compaction treatment to further improve the seismic safety of saturated loess ground.

5.4 Performance-based seismic design of anti-liquefaction treatment standard and technology of loess ground

According to the important grade of buildings and the seismic liquefaction degree of loess ground, we proposed the performance-based seismic design of anti-liquefaction treatment technology and standard of loess ground shown in Table 9.

Table 9. Treatment standards and measures of liquefaction of loess ground

Seismic liquefaction degree	Slight	Medium	Serious
Treatment standards of loess ground	II buildings	Partial elimination of liquefaction settlement	All or partial elimination of liquefaction settlement
	III buildings	No measures	Foundation and superstructure need treatment, or higher requirements
			Elimination of all liquefaction settlement All or partial elimination of liquefaction settlement and foundation and superstructure need treatment

※ I, II, III and IV buildings are the seismic fortification category of buildings based on the importance of buildings.

I buildings is the major engineering projects involving national public security and probably inducing serious secondary disasters by earthquakes with catastrophic consequence, which is special fortification. II buildings mainly refer to buildings that use functions cannot be interrupted or need to be restored as soon as possible, and will cause

significant social impact and major losses to the national economy, which is important fortification; III buildings are that have general impact after earthquake damage and other buildings that do not belong to I, II, and IV, which is regular fortification; IV buildings are that its damage or collapse will not affect people's life and slight social impact and economic loss, which is proper fortification.

The treatment techniques against loess liquefaction include soil replacement; composite foundation using cement, flyash or gravel pile; pile foundation crossing the potential liquefaction layer, and superstructure strengthening measures can be adopted to eliminating liquefaction potential and relative deformation. In addition, water proof measures are important for preventing liquefaction potential of loess ground.

5.5 Seismic design of loess pile foundation considering liquefaction

The land subsidence caused by saturated loess liquefaction lags behind the earthquake action. Therefore, considering the liquefaction of saturated loess, the seismic design of loess pile foundation should be divided into two stages: before liquefaction and after liquefaction.

Before liquefaction, the horizontal bearing capacity and horizontal displacement of piles are calculated under seismic action. The calculation diagram is shown in Fig. 14(a). According to the experimental study of pile on saturated loess ground in Gansu Province, the proportional coefficient of horizontal resistance coefficient of saturated loess is $m = 3\sim 6 \text{ MN/m}^4$, and the calculation formula of horizontal bearing capacity is:

$$H_{Eik} \leq 1.2R_{ha} \quad (4)$$

In the formula, H_{Eik} is the horizontal seismic force acting on the top of single pile under the standard combination of loads effect; R_{Eha} is the characteristic value of horizontal bearing capacity of single pile.

The control value of horizontal displacement is:

$$X_{oa} = 15\text{mm} \quad (5)$$

In the formula, X_{oa} is the allowable horizontal displacement of pile top.

After liquefaction, the horizontal seismic action is nearly zero, the liquefied soil around the pile is flowing, and the constraint effect on the pile is very small. The pile is close to the horizontal displacement column embedded in the top hinge bottom. Therefore, the stability of the pile under pressure under vertical force should be verified, and the calculation diagram is shown in Fig. 14(b).

$$N \leq \varphi\psi_a f_c A_{Pa} \quad (6)$$

Where, N is the axial pressure design value of pile top under the basic combination of load effect; φ is the stability coefficient, which can be determined according to the calculated length L of the pile and the design diameter of the pile. The calculated length of the pile can be determined according to the constraints on the top of the pile, L_0 is the free length of the surface of the stable soil layer exposed by the pile, h is the length of the pile in the stable soil layer, φ is the stability coefficient, ψ_a is the pile forming process coefficient; f_c is the design value of axial compressive strength of concrete; A_{Pa} is the cross-sectional area of the pile.

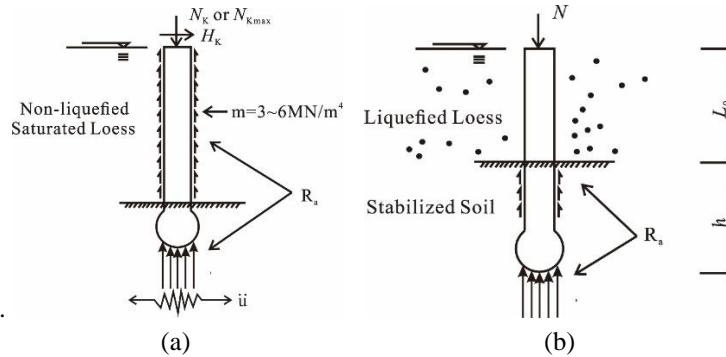


Fig. 14. Calculation diagram of loess pile foundation considering liquefaction ((a) Before earthquake; (b) After earthquake)

6 Evaluation and prevention of seismic subsidence of loess ground

6.1 Preliminary discrimination method

Based on laboratory test research, field test and on-site investigation of earthquake damage, the seismic subsidence of loess ground can be judged by loess stratum, natural water content, void ratio, dry density, soil depth, compaction coefficient, plasticity index, shear wave velocity, site predominant period and so on. The discriminant value is shown in Table 8. Generally speaking, Holocene loess (Q_4) and late Pleistocene loess (Q_3) have seismic subsidence, while the middle Pleistocene loess (Q_2) and early Pleistocene loess (Q_1) do not. The loess, which has elevated pore microstructure, natural water content higher than shrinkage limit, void ratio more than 0.8, dry density lower than 16.3kN/m^3 (or compaction coefficient less than 0.95), shear wave velocity less than 300 m/s and standard penetration number less than 18 times, may have seismic subsidence. The water content has an obvious influence on the seismic subsidence of loess. When the water content exceeds the shrinkage limit of loess (the shrinkage limit of Lanzhou loess is generally between 5.8%), the seismic subsidence of loess increases significantly with the increase of water content. The void ratio of loess is generally more than 1.0. Under the condition of optimal water content, the seismic collapsibility of compacted loess decreases with the increase of dry density, and when the dry density is higher than 16.3kN/m^3 , it is very small and may not be considered (Fig. 15). The adoption of the compaction coefficient is to provide convenience for the engineering foundation treatment, which in principle belongs to the compaction index and is related to the dry density. Compared with the seismic code, it can be seen that when the loess site is below medium-soft, it will generally have seismic subsidence, but when the site is above medium-hard, only part of the site will have seismic subsidence. Through the earth tremor test of a large number of loess sites, the predominant periods of different sites are obtained. Generally speaking, the softer the loess site is, the longer the predominant period is. When the predominant period of the loess site is less than 0.15 s, it

reflects that the soil of the site is very hard and generally does not cause seismic subsidence. PGA index is the minimum ground horizontal peak acceleration of seismic subsidence in loess site. Laboratory experiments and calculation analysis show that its value is 100 gal, and the corresponding seismic intensity is equal to 7 degrees. The on-site investigation of historical earthquakes confirmed that the seismic subsidence of loess occurred in the area with intensity above 7 degrees. The lower limit depth of earthquake subsidence soil layer reflects that when the loess soil layer is buried deep, its structure is relatively stable and earthquake subsidence is not easy to occur.

Table 8. Initial judgement index of seismic subsidence of loess

Initial Judgement Index	Layer	Microstructure Type	W(%)	e	$\gamma_d(\text{kN/m}^3)$	Compaction Coefficient
Discriminant Value of Seismic Subsidence	Q_3, Q_4	elevated pore microstructure	$>W_s$	>0.8	<16.3	<0.95
Initial Judgement Index	$V_s(\text{m/s})$	Predominant Period	PGA(gal)	Soil Depth	Number of Standard Penetration Hits	Plasticity Index
Discriminant Value of Seismic Subsidence	≤ 200	≥ 0.15	≥ 100	≤ 20	< 18	< 15

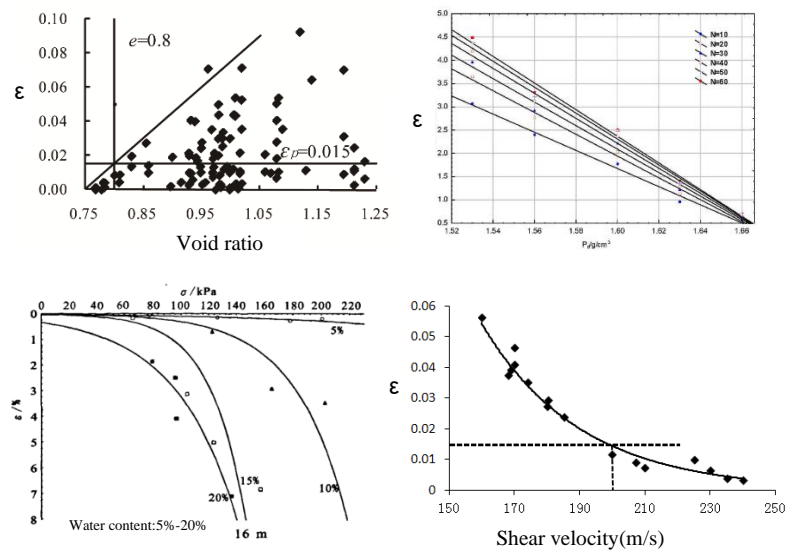


Fig. 15. The relationships between seismic subsidence coefficient and void ratio, dry density, water content, and shear velocity.

The above indexes are usually on the safe side. However, for the projects of different importance, it is still necessary to adopt reasonable principles when using the above initial judgment indexes to distinguish the site seismic subsidence. It is suggested that for III and IV buildings with no more than 10 storeys, if the above discriminant indexes reach the standard of non-seismic subsidence soil, the problem of seismic subsidence may not be considered. However, for important projects, high-rise buildings and other sites with big additional stress, it is necessary to reach at least two relatively independent indexes at the same time in order to judge that the loess site does not have seismic subsidence. Otherwise, a special research and evaluation should be carried out.

6.2 Detailed discrimination method

The detailed discrimination of seismic subsidence of loess ground can be carried out by dynamic triaxial tests. The seismic subsidence coefficient is defined as the residual strain, $\varepsilon_p(N)$, under a certain cyclic times (N) shown as formula (7):

$$\varepsilon_p(N) = \frac{h_0 - h_1(N)}{h_0} \quad (7)$$

Where, $\varepsilon_p(N)$ is seismic subsidence coefficient (%); h_0 denotes the height of a specimen before applying dynamic loading (mm); $h_1(N)$ denotes the height of a specimen after applying dynamic loading (mm). Based on dynamic triaxial tests, $\varepsilon_p(N)$ can be determined by the recorded time histories of dynamic axial stress and strain shown as Fig.16 (a). Through a series of dynamic triaxial tests with a certain confining stress for 4-5 specimens to be subjected to different amplitudes of dynamic stress, the curves of dynamic stress, σ_d , versus residual strain, ε_p (seismic subsidence coefficient), can be figured out (Fi.16(b)).

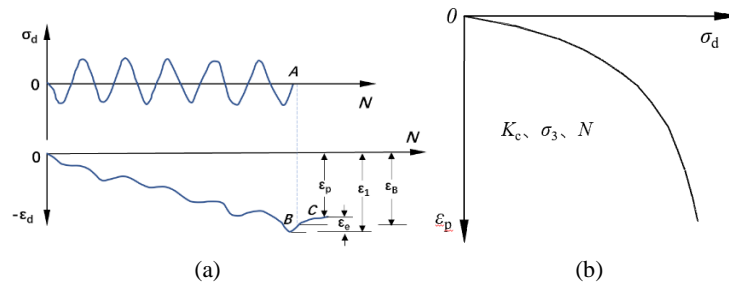


Fig.16. The diagram of determination of seismic subsidence coefficient ((a) The recorded time histories of dynamic axial stress and strain; (b) the curves of dynamic stress versus seismic subsidence coefficient).

The quantity of cumulative seismic subsidence of loess ground can be calculated by the formula (8)

$$Sd = \sum \Delta h_i^* \varepsilon_{pi} \quad (8)$$

Where, S_d is the quantity of cumulative seismic subsidence of loess ground under a certain fortification PGA; Δh_i is the thickness of loess layer i ; and ε_{pi} denotes the seismic subsidence coefficient of loess layer i . Seismic subsidence of loess ground are evaluated with 3 grade, light, medium, serious, according to the value of S_d under a certain fortification PGA shown as Table 9. Thus, loess ground can be evaluated according to its accumulative quantity of seismic subsidence under a certain fortification PGA: $0 < S_d \leq 20$ cm, slight seismic subsidence; $20\text{cm} < S_d < 80$ cm, medium seismic subsidence; $S_d > 80\text{cm}$, serious seismic subsidence.

Table 9. The detailed discrimination of seismic subsidence of loess ground

Seismic subsidence grade	Slight	Medium	Serious
$S_d(\text{cm})$	$0 < S_d \leq 20$	$20 < S_d \leq 80$	$S_d > 80$

6.3 Technology and standard of anti- subsidence treatment of Loess ground

Dynamic compaction method (DCM)

The dynamic triaxial tests of loess seismic subsidence at the depths of 4 meters in 3000 kN•m tamping area and 2 m, 4 m and 6 m in 6000 kN•m tamping area were carried out respectively, and compared with the seismic subsidence test of undisturbed loess before treatment. The result is shown in Fig. 17. It shows that the seismic subsidence curve of loess in the effective depth range of dynamic compaction changes from non-linear to linear after dynamic compaction. No matter 3000 kN•m or 6000 kN•m energy level dynamic compaction, the seismic subsidence coefficient is less than 0.01(1%) under the action of dynamic stress of 220 kPa. And with the increase of dynamic stress, the increase of seismic subsidence coefficient decreases. After dynamic compaction, the seismic subsidence coefficient of loess does not increase with the increase of cyclic times. The residual strain mainly occurs in the first 10 cyclic times, and then increases more slowly with the increase of cyclic times, and the seismic subsidence curve is very close.

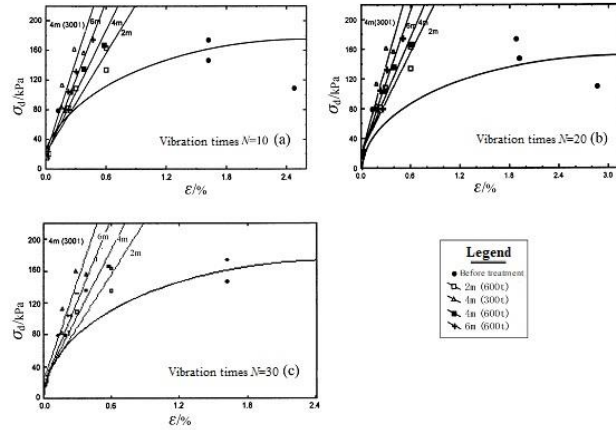


Fig. 17. Seismic subsidence curve of loess site before and after dynamic compaction

To sum up, the method of dynamic compaction to deal with the collapsibility of loess ground can completely eliminate the seismic subsidence under the optimal water content in the range of effective depth. The dry density of the treatment should be increased with water content. The dry density standard should be 1.63 g/cm^3 at the optimal water content (about 16%). This value can be reduced at a lower water content, but it has to be determined according to the water content.

Compaction pile method (CPM)

The research site is the first Primary School of Lanzhou Refinery and the No.15 Depot of Lanzhou Grain Depot Reconstruction and extension Project directly under the State Grain Reserve Bureau. Lime-soil compaction piles are used to eliminate the collapsibility of loess in the range of 9m and 7m respectively. The filling material in the hole is lime-soil at 2:8. The length of lime-soil pile is 9 m and 7 m respectively, and the diameter of the pile is 400 mm, and the distance between piles is 1 m. The technology of pile sinking is adopted. The backfill height of each layer of lime soil is 100 cm, which is compacted by layers. After treatment, the collapsibility of loess is eliminated in the depth of 9 m and 7 m respectively.

It can be seen from Fig. 18 that due to the improvement of the treatment standard of lime-soil compaction pile, the compactness of ground loess has been greatly increased, and the seismic subsidence curve has changed from a nonlinear curve to an approximate straight line. The seismic subsidence of loess within 7 m depth has been eliminated. This shows that under certain conditions, to improve the standard of collapsibility treatment of loess ground by lime-soil compaction pile, while collapsibility is eliminated, seismic subsidence can also be eliminated. However, by comparing the results of the first section, it can be found that the seismic subsidence coefficient under 200 kPa is still larger than that under static state. The former is about 0.012 and the latter is 0.004. Therefore, the treatment of seismic subsidence of loess ground should consider the intensity of ground motion that may be suffered in the future.

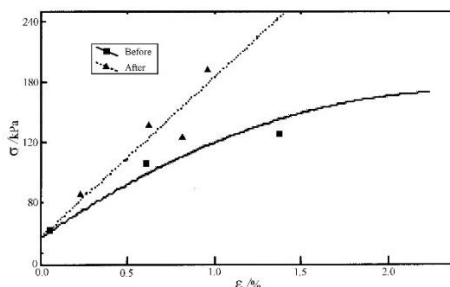


Fig. 18. Comparison of seismic subsidence of loess ground before and after lime-soil compaction pile treatment

6.4 Performance-based seismic design of anti-seismic subsidence treatment technology and standard of loess ground

According to the important grade of buildings and the seismic subsidence degree of loess ground, we proposed the performance-based seismic design of seismic subsidence treatment technology and standard of loess ground. The contents are shown in table 10.

Table 10. Treatment measures of seismic subsidence of loess ground

Seismic subsidence grade	Slight	Medium	Serious
Treatment methods	No measures	The collapsibility and seismic subsidence of loess ground should be considered together in the design, and comprehensive measures combining ground treatment, waterproof measures and structural measures should be taken.	
Treatment standard	II buildings	The whole or local cushion, dynamic compaction and other composite foundation shall be used to eliminate all or part of the settlement of the ground, or the pile foundation shall be used to transfer the building load to the deeper non-collapsible and non-seismic subsidence soil layer.	
	III Buildings	No measures	No measures

6.5 Seismic calculation of loess pile foundation considering seismic subsidence

We carried out a large-scale field tests and observation for negative friction resistance of large-diameter concrete cast-in-situ piles (pile diameter 0.8 m, length 20 m) in Q3 loess ground with seismic subsidence induced by blasting simulation in the southern

margin of Lijiawanping, Lintao County, Gansu Province[34]. The measured results show that:

(1) The maximum seismic subsidence of loess site is 33 mm, which is far less than that of soil settlement when loess site is immersed and collapsible. However, the average negative friction stress is 54 kPa, and the corresponding total negative friction force is 1654 kN, which is much larger than the observed value of negative friction under loess collapsibility. Therefore, the negative friction caused by seismic subsidence of large-diameter concrete cast-in-place pile foundation in unsaturated loess area can not be ignored

(2) The seismic subsidence of loess below 20 m in Q₃ loess layer is negligible.

The large-diameter concrete pile foundation on Q₃ loess ground should consider the two situations that is before and after the earthquake to carry out the seismic calculation of the pile foundation.

Before earthquake, the calculation diagram is shown in Fig. 19(a). The design criterions are presented in formula (9) and (10).

$$N_k \leq 1.2R_a \quad (9)$$

$$N_{k\max} \leq 1.2R_a \quad (10)$$

In the formulae, N_k is the average vertical force of single pile under the axial vertical force of standard combination of load effect; $N_{k\max}$ is the maximum vertical force of pile top under eccentric vertical force of standard combination of load effect; R_a is the characteristic value of vertical bearing capacity of single pile.

After earthquake, the calculation diagram is shown in Fig. 19(b). The design criterions are presented in formula (11) and (12).

$$N_{EK} + Q_g^n \leq 1.25R_a \quad (11)$$

$$N_{EK\max} + Q_g^n \leq 1.5R_a \quad (12)$$

In the form, N_{EK} is the average vertical force of single pile under the standard combination of seismic effect and load effect; $N_{EK\max}$ is the maximum vertical force of single pile under standard combination of seismic effect and load effect; Q_g^n is the pull-down load of single pile caused by negative friction.

Drawdown loads of negative friction pile foundation based on experimental results:

$$Q_g^n = u \cdot q_{sk}^n \cdot L_s \quad (13)$$

In the formula, u is the perimeter of the pile (m); q_{sk}^n is the average negative friction characteristic value (kPa) of single pile under seismic subsidence; L_s is the thickness of loess layer (m).

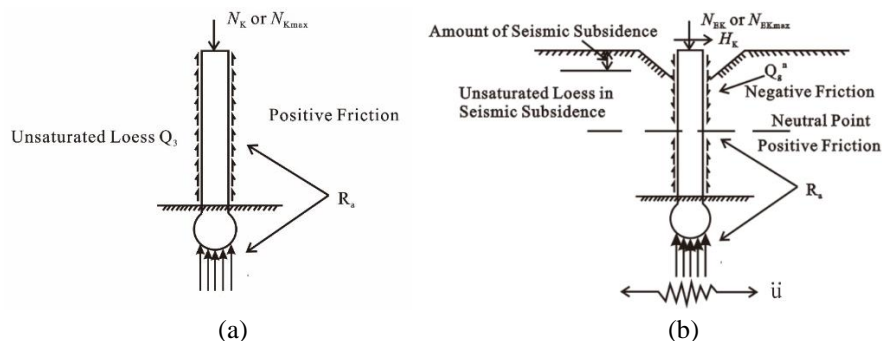


Fig. 20. Calculation diagram of loess pile foundation considering seismic subsidence ((a) Before earthquake; (b) After earthquake)

7 Conclusions

Loess is a kind of silt dominated special soil with porous microstructure and weak cementation, which makes it have high seismic vulnerability and water sensitivity. Loess Plateau is a strong earthquake-prone region, where large casualties were caused by earthquakes. Large casualties attributed to a large scale of landslides, liquefaction, seismic subsidence and amplification of ground motion at loess sites.

The distribution of the three kinds of geotechnical disasters has the similarity of overall trend. The most serious loess earthquake disasters involve in Ningxia, Gansu, Shaanxi and Shanxi provinces. The region with lower risk of loess earthquake disasters is Ordos block.

The amplification effect of deposit thickness and topography of loess sites in the Loess Plateau on seismic ground motion is remarkable, which may amplify PGA by 1.1–2.2 times of the value at rock base and predominately elongate characteristic period. In seismic design of engineering loess sites, it should be into account.

The risk assessments of seismic landslides and seismic design methods for engineering loess slopes with single-step and multi-steps are provided. The distance between the building and the edge of the slope crest and the distance between the edge of the foundation slab and the edge of the slope bottom should be determined by the type of building and the height of slope.

The preliminary discrimination and detailed discrimination methods of evaluating liquefaction and seismic subsidence of loess sites and its treatment measurements are respectively presented. Seismic treatment standards of loess ground should be adopted based on the importance of buildings and grade of liquefaction and subsidence of loess ground.

The pile foundation design considering seismic subsidence in unsaturated loess ground and liquefaction in saturated loess ground should distinguish before and after the earthquake. The vertical bearing capacity of pile foundation should consider the negative friction caused by seismic subsidence after the earthquake. The stability of the pile without surrounding soil constraints shall be checked in liquefied loess ground after the earthquake.

8 Acknowledgment

This research work is financially supported by the Key Project of National Natural Science Foundation of China (No. U1939209)

References

1. Prakash S., Puri V.K. Liquefaction of loessial soils. Third International Conference on Seismic Microzonation, pp. 1101-1107. Seattle, USA (1982).
2. Prakash S., Sandoval J. A. Liquefaction of low plasticity silts. *Journal of Soil Dynamics and Earthquake Engineering* 71(7), 373-397 (1992).
3. Prakash S., Guo. T. Liquefaction of silts and silt-clay mixtures. *Geotechnical Earthquake Eng. and soil Dynamics III*, ASCE, pp337-346, Seattle, Wash (1998).
4. Ishihara K., Okuss S., Oyagi N., Ischuk A. Liquefaction-induced flow slide in the collapsive loess deposit in Soviet Tajik. *Soils and Foundations* 30(4), 73-89 (1990).
5. Xie DY. *Soil dynamics*. Xi'an Jiaotong University Press, Xi'an (1988).
6. Xie DY., Zhang YH. The influence of coupling change of static stress on the development law of pore water pressure under dynamic load. *Proceedings of the 4th National Academic Conference on soil dynamics*, pp13-20. Zhejiang University Press, Hangzhou (1994).
7. Wu ZH., Fang Y. Seismic subsidence characteristics of undisturbed loess during humidification. *Proceedings of the third National Soil Dynamics Conference*, Tongji University Press, Shanghai (1990).
8. Duan RW. Experimental study on dynamic characteristics of Lanzhou loess. *Journal of Northwest seismology* 1(2), 43-49 (1979).
9. Duan RW., Zhang ZZ., Li L., Wang Jun. Further study on dynamic characteristics of loess. *Journal of Northwest seismology* 12(3), 72-78 (1990).
10. Wang J., Wang LM., Li L. Effects of different seismic loads on dynamic modulus and damping ratio of loess. *Journal of natural disasters* 1(4), 75-79 (1992).
11. Wang LM., Zhang ZZ., Wang Jun., Li Lan. Test method for dynamic strength of loess under random seismic load. *Journal of Northwest seismology* 13(3), 50-55 (1991).
12. Wang LM., Zhang ZZ., Wang J., Li Lan. Experimental study on dynamic constitutive relationship of loess under random seismic load. *Journal of Northwest seismology* 14(3) 61-68 (1992).
13. Hu RL., Li ZF., Wang SJ., Zhang LZ., Li XQ. Study on strength characteristics and structural change mechanism of loess under dynamic load. *Journal of geotechnical engineering* 22(2), 174-181 (2000).
14. Shi YC., Zheng MJ. Characteristics of dynamic shear modulus and damping ratio of loess in Northwest China. *Journal of Northwest seismology*, 19 144-150 (1997).
15. Zhang ZZ., Sun CS., Duan RW., Wang LM. *Loess earthquake disaster prediction*. Seismological Publishing House, Beijing (1999).
16. Liu BC., Zhou JX., Li QM. Interpretation of aerial photos of Tongwei earthquake in 1718 and Tianshui earthquake in 1654. *Earthquake science research* (1), 1-9 (1984).
17. Chen BW., Zhang JS. Problems of earthquake engineering geology of loess sites and their estimating methods. In: *Aspects of Loess Research*. China Ocean Press, 403-409 (1987).
18. He G., Zhu HB. Study on seismic subsidence of loess *Journal of geotechnical engineering* 17(6), 99-103 (1995).

19. Huang YH. Application of random search method for the most dangerous slip surface of soil slope in earthquake landslide disaster prediction. Proceedings of the Fourth National Academic Conference on soil dynamics, Zhejiang University Press, Hangzhou (1994).
20. Wang LM., Wang J., Li L., Shi XF., Wu JH. Prediction method of liquefaction of urban loess site Journal of Northwest seismology 19,7-12 (1997).
21. Wang LM., Yuan ZX., Shi YC., Sun CS. Study on indexes and methods of seismic disaster zoning in loess Journal of natural disasters 8(3), 87-92 (1999).
22. Wang LM., Yuan ZX., Wang J., Sun CS. Influence of dry density on seismic subsidence of compacted loess Earthquake engineering and engineering vibration 20(1), 75-80 (2000).
23. Wang LM., Liu HM., Li L., Sun CS. Experimental study on liquefaction mechanism and characteristics of saturated loess. Journal of geotechnical engineering 22(1), 89-94 (2000).
24. Zou JC., Shao SM. Fuzzy comprehensive evaluation of landslide distribution law in Gulang Haiyuan area. Journal of Seismology 1, 1-6 (1994).
25. Zou JC., Shao SM. Gulang earthquake landslide and its relationship with fault zone. Journal of Northwest seismology 16(3), 60-64 (1994).
26. Zou JC., Shao SM. Discussion on Haiyuan earthquake landslide and its distribution characteristics. Inland earthquake 10(1), 1-6 (1996).
27. Sun CS., Cai HW. Development and distribution characteristics of landslide and collapse geological disasters during historical earthquakes in China. Journal of natural disasters 6(1), 25-30 (1995).
28. Qin HY. Research and Discussion on high speed loess landslide induced by earthquake, Soil dynamics and geotechnical earthquake engineering, pp236-246. China Construction Industry Press, Beijing (2002).
29. Bai MX., Zhang SM. Liquefaction movement of loess stratum during high intensity earthquake. Engineering Investigation, (6):1-5 (1990).
30. Wang JD., Zhang ZY. Study on Mechanism of earthquake induced high speed loess landslide. Journal of geotechnical engineering 21(6), 670-674 (1999).
31. Liu HL., She YX., Wang LM. Experimental study on liquefaction of dynamic compaction loess ground. The 6th National Conference on soil dynamics pp 218-224. China Construction Industry Press, Beijing (2002).
32. She YX., Liu HL., Wang LM. Experimental study on pore water pressure growth model of loess The 6th National Conference on soil dynamics, pp 225-230. China Construction Industry Press, Beijing (2002).
33. Wang GH. Study on liquefaction of the sandy soil mixed with loess. Proceedings of Fourth International Conference on Recent Advances in Geotechnical Earthquake Engineering and Soil Dynamics, University of Missouri-Rolla, Paper No.4.37, San Diego, USA (2001).
34. Wang LM, Sun JJ, Huang XF, Xu SH, Shi YC, A field testing study on negative skin friction along piles induced by seismic subsidence of loess, Soil Dynamics and Earthquake Engineering, 31, pp 45-58(2011).